BRAIN. Broad Research in Artificial Intelligence and Neuroscience
e-ISSN: 2067-3957 | p-ISSN: 2068-0473
Covered in: Web of Science (ESCI); EBSCO; JERIH PLUS (hkdir.no); IndexCopernicus; Google Scholar; SHERPA/RoMEO; ArticleReach Direct; WorldCat; CrossRef; Peeref; Bridge of Knowledge (mostwiedzy.pl); abcdindex.com; Editage; Ingenta Connect Publication; OALib; scite.ai; Scholar9; Scientific and Technical Information Portal; FID Move; ADVANCED SCIENCES INDEX (European Science Evaluation Centre, neredataltics.org); ivySCI; exaly.com; Journal Selector Tool (letpub.com); Citefactor.org; fatcat!; ZDB catalogue; Catalogue SUDOC (abes.fr); OpenAlex; Wikidata; The ISSN Portal; Socolar; KVK-Volltitel (kit.edu)
2026, Volume 17, Issue 3, pages: 349-368
Submitted: April 25th, 2026 | *Accepted for publication:* August 22nd, 2026

Quality-Controlled Pipeline for Multi-Segment Wearable Accelerometry in Physiological and Pathological Gait Assessment

Marius Dobîndă-Albu
Faculty of Physics, Alexandru Ioan Cuza University of Iași, Bulevardul Carol I No. 11, 700506 Iasi, Romania.
marius.dobinda@student.uaic.ro;
marius.dorin3@gmail.com,
https://orcid.org/0009-0000-4951-8562

Abstract: *Wearable accelerometry brings gait assessment closer to clinical feasibility. Recording quality and unequal signal duration can still influence between-group comparisons. This study evaluated a quality-controlled, bilateral, multi-segment accelerometry pipeline in 31 participants (15 with pathological gait and 16 with physiological gait) who walked 30 m at a self-selected pace. Six triaxial accelerometers recorded bilateral acceleration at the hip, knee, and ankle levels, and identical analyses were performed using an up-to-30-s window and a fixed 15-s window. Eight of ten focused descriptors met the predefined robustness criteria in both configurations. The physiological group showed higher knee, ankle, and combined knee–ankle RMS, higher ankle and combined knee–ankle dominant frequency, and higher estimated accelerometric cadence. The pathological group, in turn, showed greater knee and ankle RMS asymmetry. High-frequency ratios and global DFA exponents were not statistically significant after false-discovery-rate correction. These group-level findings support explicit quality control and temporal sensitivity analysis in wearable gait assessment, but they cannot be attributed exclusively to pathology because the groups were not age-matched and walking speed was not independently measured. Individual clinical interpretation requires external validation.*

Keywords: *wearable accelerometry; gait analysis; pathological gait; neurological gait; bilateral asymmetry; quality control; temporal sensitivity analysis.*

How to cite: Dobîndă-Albu, M. (2026). Quality-controlled pipeline for multi-segment wearable accelerometry in physiological and pathological gait assessment. *BRAIN. Broad Artificial Intelligence and Neuroscience*, *17*(3), 349-368. https://doi.org/10.70594/brain/17.3/21

1. Introduction

Although gait appears to have a periodic structure, stride-to-stride fluctuations contain meaningful temporal organisation rather than representing measurement noise alone (Goldberger et al., 2002; Hausdorff, 2007; Hausdorff et al., 1995). Wearable accelerometry can additionally characterise gait through time- and frequency-domain features related to movement amplitude and rhythm (Hsu et al., 2021; Sejdić et al., 2014), while bilateral measurements can provide information on between-limb asymmetry (Anwary et al., 2018).

Neurological disorders can affect gait by altering the control of the lower limbs. These changes may be reflected in reduced acceleration amplitude, altered rhythm, increased asymmetry, or changes in the temporal structure of the recorded signal.

Clinical observation and the analysis of spatiotemporal parameters have traditionally constituted the main approaches to gait assessment. Modern technologies, such as force platforms and optoelectronic motion-analysis systems, enable detailed and precise measurements but require specialised infrastructure, trained personnel, and controlled laboratory conditions. These requirements may limit their repeated use in clinical practice and the assessment of overground walking under conditions similar to those encountered in rehabilitation settings.

1.1. Literature Review

In this context, wearable inertial sensors have become increasingly important because they enable movement recording during overground walking and can be more easily integrated into clinical assessment and rehabilitation programmes (Chen et al., 2016; Díaz et al., 2020). However, many systems use a single measurement location or a limited number of sensors. Such configurations are useful for estimating global gait parameters but provide limited information regarding the regional distribution of accelerations and the differences between homologous segments of the two lower limbs.

The bilateral placement of sensors at the hip, knee, and ankle levels may enable a comparative characterisation of proximal and distal acceleration patterns without reducing the entire locomotor process to a single signal.

An additional difficulty arises when recordings are obtained under clinically feasible conditions during overground walking performed at a self-selected speed. Participants with pathological gait may take a different amount of time to cover the same distance compared with the reference group, leading to different recording durations. Also, wearable recordings can be affected by acquisition-related problems that influence file completeness or numerical integrity. Under these conditions, between-group differences may be influenced not only by gait characteristics but also by the duration of the analysed segment or by acquisition-related problems.

For this reason, a comparative analysis based on wearable sensors requires explicit quality-control procedures, identical processing of all channels, and verification of the results using comparable temporal windows. This issue is particularly important for nonlinear descriptors, including Detrended Fluctuation Analysis (DFA), whose estimates may depend substantially on the length of the analysed time series (Mohammadzadeh Gonabadi & Burnfield, 2026).

Accelerometric signals recorded during walking can be described using several complementary categories of parameters. Root mean square (RMS) values characterise acceleration amplitude, whereas spectral analysis enables the identification of the dominant rhythmic component and the estimation of the contribution of higher-frequency components. Cadence can be estimated from gait-related events detected in distal acceleration signals, whereas differences between left- and right-side values can be used to quantify between-limb asymmetry. These descriptors characterise movement intensity, rhythm, and bilateral asymmetry but do not fully describe the temporal organisation of fluctuations. Detrended Fluctuation Analysis can be used to characterise scaling properties in non-stationary time series (Peng et al., 1994). In gait research, DFA has commonly been applied to stride-interval time series, and its estimates depend on methodological choices, including series length and analysis parameters (Phinyomark et al., 2020). For continuous

segmental acceleration signals, the DFA exponent should therefore be interpreted as a scaling slope specific to the analysed signal and scale range rather than as a direct equivalent of the Hurst exponent obtained from stride-interval series.

1.2. Research Gap, Objectives, and Contribution

The present study evaluates a quality-controlled multi-segment accelerometric data-processing pipeline for the comparative analysis of physiological and pathological gait.

Signals were recorded using GaitFlow Scanner, an STM32-based system previously presented elsewhere (Dobîndă-Albu, 2026), which uses six triaxial ADXL345 accelerometers placed bilaterally at the hip, knee, and ankle levels. For each participant, 18 acceleration time series were acquired within the same centralised acquisition loop. The pipeline integrated file-structure verification, identical processing of all channels, calculation of dynamic acceleration magnitude, and extraction of descriptors related to amplitude, rhythmicity, spectral content, asymmetry, estimated cadence, and global DFA scaling.

The primary objective of the study was neither to define diagnostic criteria nor to validate a single descriptor as a biomarker of pathological gait. Instead, the study aimed to determine whether a quality-controlled multi-segment accelerometry pipeline could identify interpretable between-group differences and whether the direction and magnitude of these contrasts were maintained when the analysis was repeated using two predefined temporal windows.

The contribution of this article consists of the cohort-level application of a bilateral six-sensor accelerometric configuration, the integration of file-level quality control, and the identification of descriptors that remain significant after false-discovery-rate (FDR) correction, show large effect sizes, and preserve the same direction in the 30 s and 15 s analyses.

2. Materials and Methods

2.1. Study Design and Participants

This was an observational and methodological study. The purpose was to evaluate whether a multi-segment accelerometric pipeline could identify interpretable and robust differences between physiological and pathological gait. The final analysis was based on a quality-controlled dataset including 31 participants: 15 with pathological gait and 16 with physiological gait.

The pathological group consisted of participants whose neurological conditions—post-stroke unilateral hemiparesis (n = 7), post-stroke unilateral hemiplegia (n = 5), Parkinson's disease (n = 2), and spastic paraparesis (n = 1)—affected lower-limb control during walking and overall gait performance. Among the 12 post-stroke participants, the affected side was right in eight participants and left in four. The physiological group included adults with no known neurological or musculoskeletal condition and no observable gait impairment, as determined by clinical observation without the use of a standardised gait-screening instrument. Recordings from this group served as a comparison reference for physiological overground gait under the same experimental conditions, not as a normative database.

For the pathological group, participants were included if they had a neurological condition that affected gait and if they were able to complete the proposed 30-m overground walking task, with or without the participant's assistive device. Exclusion criteria for this group were severe musculoskeletal conditions or other medical conditions that could independently and substantially affect gait, acute cardiovascular conditions, cognitive impairment preventing the understanding of simple instructions, or the inability to complete the walking task safely.

For the physiological group, the inclusion criteria were the absence of any neurological or musculoskeletal conditions that could affect gait performance, no observable gait impairment based on clinical observations, and the ability to complete the same walking task. Exclusion criteria for this group were any neurological condition, musculoskeletal or other medical condition that could

affect gait, observable gait impairment, cognitive impairment preventing the understanding of simple instructions, or inability to complete the walking task safely.
No standardised functional-status scale was administered. The recordings were obtained on the same indoor path and with the same acquisition system in order to reduce the influence of methodological differences between groups.

Assistive devices (canes or crutches) were allowed in the pathological group when they represented a participant's habitual mode of walking or were needed to walk the proposed distance safely. During the recorded trial, 9 participants walked without an assistive device, one participant used a cane, and 5 participants used one crutch each. All assistive devices were used contralateral to the affected limb.

The final dataset included 15 participants (9 men and 6 women) in the pathological group and 16 participants (8 men and 8 women) in the physiological group. The pathological group had a higher median age than the physiological group, 59 [52–65] years versus 48 [38.5–55.75] years. This age difference was treated as a contextual factor and a possible confounder, not as a primary biomechanical finding.

Some participants included in the present study had also participated in previous work involving the GaitFlow system (Dobîndă-Albu, 2026). The recordings analysed here were acquired separately and were not used in that publication. The present study addresses a distinct methodological question through a quality-controlled triaxial-magnitude pipeline, conventional accelerometric descriptors, temporal-window sensitivity analysis, and FDR-controlled between-group comparisons.

Written informed consent was obtained before data acquisition. The experimental protocol was approved by the Ethics Committee of “Sf. Gheorghe” Rehabilitation Hospital, Botoșani, Romania, under approval no. 1/14.02.2025.

2.2. Wearable Accelerometric Acquisition System

Lower-limb acceleration signals were recorded using GaitFlow Scanner, a custom-built wearable acquisition system previously described elsewhere (Dobîndă-Albu, 2026). The acquisition unit was based on an STM32F411 microcontroller connected to six triaxial ADXL345 accelerometers. The six accelerometers were bilaterally attached during gait recording using rigid fixation straps with hook-and-loop (Velcro) closures. The hip-level sensors were placed on the lateral side of the pelvis, approximately at the iliac crest level and above the greater trochanter; therefore, their signals mainly represented the acceleration of the pelvic segment. Sensors were placed over the anterior aspect of the distal thigh just superior to the patella at the level of the knee. The ankle-level sensors were placed on the anterior surface of the distal lower leg, just above the line of the talocrural joint. At each anatomical level, sensor placement, orientation, and fixation were kept consistent across participants (Figure 1a).

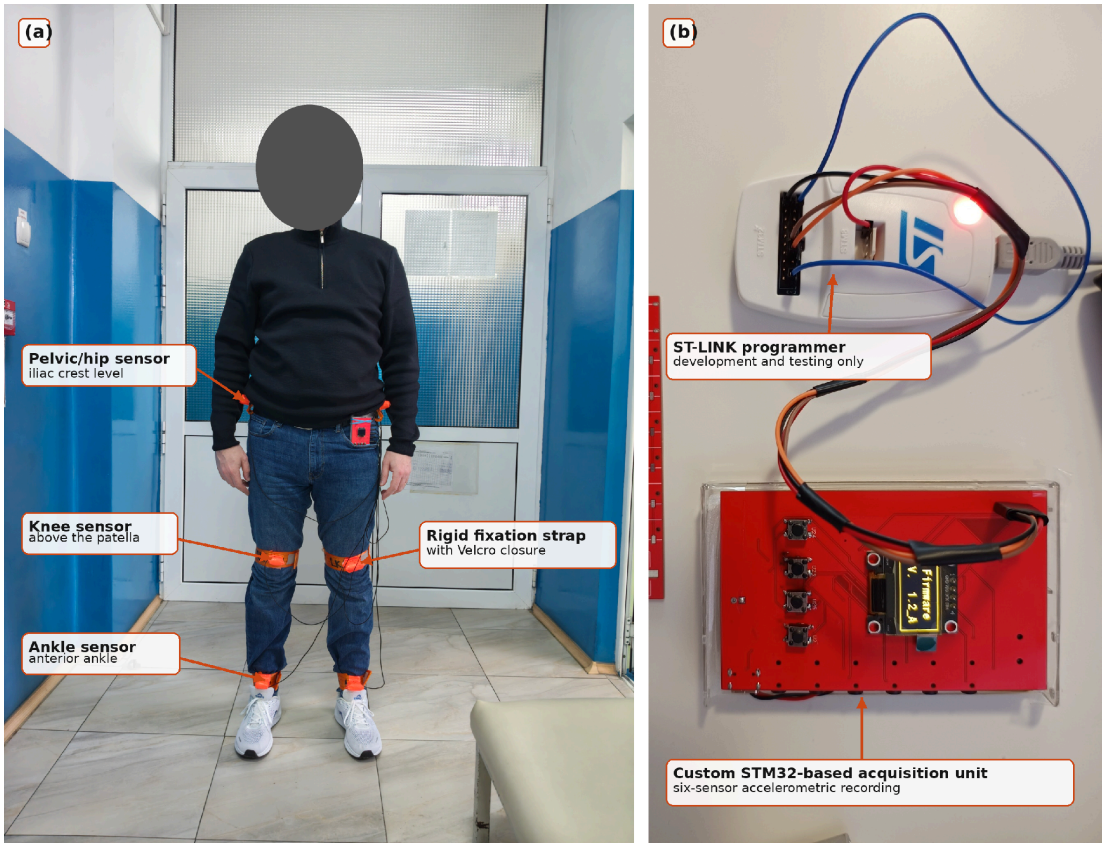

Figure 1. GaitFlow Scanner wearable accelerometry system. (a) Six-sensor configuration used during system development and testing, with accelerometers positioned bilaterally at the hip, knee, and ankle levels and secured with rigid fixation straps with hook-and-loop (Velcro) closures. The person shown is the author and not a study participant. (b) STM32-based acquisition unit used to record synchronised data from six triaxial accelerometers.

Each complete frame contained three acceleration components from each of the six sensor locations, resulting in 18 temporally aligned acceleration channels for every participant. This configuration preserved regional information from the hip, knee, and ankle levels, as well as bilateral information required for left–right comparisons.

The system was used exclusively for signal acquisition and storage. It did not provide real-time feedback, automatic classification, or clinical decision support. All preprocessing, descriptor extraction, quality-control procedures, and statistical analyses reported in this study were performed offline using dedicated Python scripts.

2.3. Walking Protocol

The experimental protocol consisted of overground walking along a 30 m indoor path, with no direction changes and no obstacles. Participants were asked to walk the path at their usual comfortable pace, without a prescribed cadence, walking speed, or a fixed path duration.

The same general protocol was applied to both groups. For participants with gait impairments, assistive devices were used when needed for safe ambulation and when they matched the participant's habitual walking mode.

Because walking was self-paced, recording duration varied between participants and was treated as contextual information rather than analysed as a primary biomechanical outcome. Walking speed was not independently measured; therefore, recording duration was not used as a substitute for a direct gait-speed measurement.

2.4. Raw Data Structure

For each walking trial, the acquisition unit generated a text file containing 18 numerical columns. This structure resulted from the six triaxial accelerometers, ordered in the data file as follows: left hip, right hip, left knee, right knee, left ankle, and right ankle. For each sensor, the three recorded components corresponded to the X, Y, and Z axes. The same ordering was used by the acquisition software and the offline analysis pipeline.

The three axes were interpreted according to a common anatomical convention applied to all sensor locations. The X axis was defined as medio-lateral, the Y axis as antero-posterior, and the Z axis as vertical. X represents lateral oscillation; Y represents forward progression; Z represents vertical acceleration.

Acceleration values stored in the raw text files were expressed in units of gravitational acceleration (g). No conversion to m/s² was applied in the offline pipeline. Because subsequent preprocessing involved mean centring, linear filtering, and calculation of the triaxial Euclidean magnitude, the dynamic acceleration magnitude and its RMS retained the same unit (g).

Participant information was encoded directly in the file name. The naming structure included the participant code, sex, and age, and these elements were extracted automatically by the Python scripts before descriptor calculation. File names followed patterns such as PT001_SF_65.txt and CF001_SM_45.txt, where "PT" denoted the pathological group, "CF" the physiological group, "SF" female sex, "SM" male sex, and the final value represented the participant's age.

Raw files lacked timestamps, so recording duration was calculated from the number of valid complete frames using an effective system frame rate of approximately 310 frames/s. Each row represented one complete frame containing 18 acceleration values from the six triaxial accelerometers. The effective frame rate was determined during firmware testing of the six-sensor configuration and was used to adjust the acquisition timing to the actual rate of approximately 310 complete frames per second.

2.5. File Quality Control

Before descriptor extraction, a quality-control pass was performed using a dedicated Python script that read files line-by-line and flagged non-conforming lines. All lines were counted for quality-control purposes, while only valid numerical lines were retained for analysis. For each file, the following were checked: file name structure; group membership; sex and age extracted from the name; number of columns; total number of lines; number of valid numeric lines; number of corrupted lines; number of lines with an incorrect column count; total recording duration; and duration available for analysis.

Only valid numeric lines with 18 columns were accepted for analysis, and each file was assigned one of three statuses: GOOD, ACCEPTABLE, or REJECT.

GOOD files met the structural, duration, and numerical integrity requirements. ACCEPTABLE files were usable for analysis but presented minor limitations, such as a duration shorter than the nominal analysis window or corrupted lines with no impact on numerical processing. Files containing fewer than 15 s of valid data or a structure incompatible with the predefined acquisition format were classified as REJECT.

No file in the final dataset of 31 participants was rejected. Every file was retained in the final analysis and was classified as either GOOD or ACCEPTABLE.

2.6. Analysis Windows

Analysis was performed using two temporal configurations. The primary analysis examined up to 30 s of valid data. Files longer than 30 s were analysed using only the first 30 valid seconds, whereas files shorter than 30 s were analysed over their complete valid duration, provided that the minimum required duration of 15 s was available.

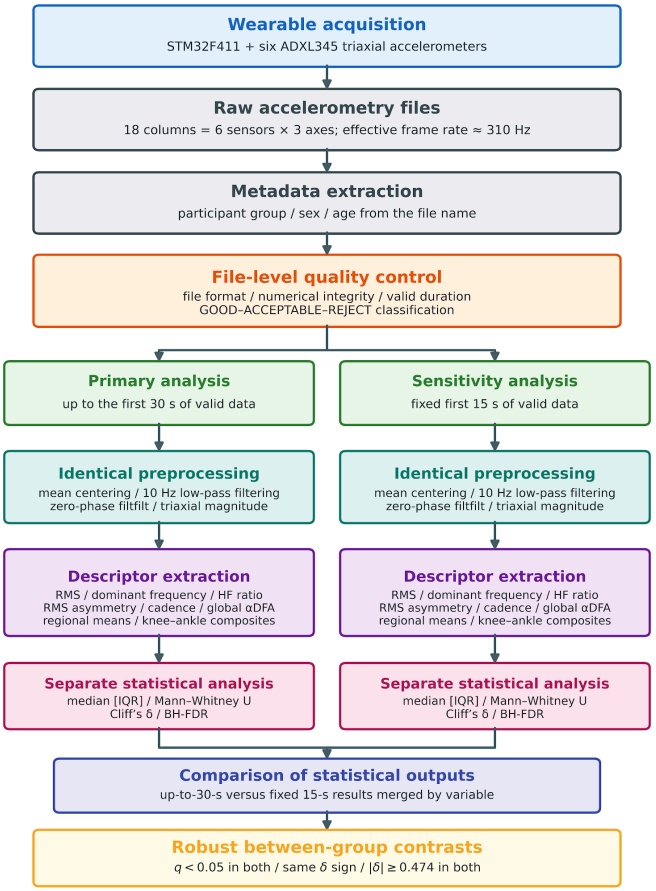

Figure 2. Overview of the quality-controlled multi-segment wearable accelerometry pipeline. Following metadata extraction and file-level quality control, each recording was processed independently using an up-to-30-s primary configuration and a fixed 15 s sensitivity configuration using the first 15 s of valid data. Identical preprocessing, descriptor extraction, regional aggregation, and statistical analyses were applied to both datasets. Statistical outputs were subsequently compared by variable, and between-group contrasts were classified as robust when they remained significant after FDR correction in both analyses, showed the same sign of Cliff's delta, and exhibited a large effect in both temporal configurations. RMS, root mean square; HF, high-frequency; IQR, interquartile range; BH, Benjamini–Hochberg procedure; FDR, false discovery rate; DFA, Detrended Fluctuation Analysis.

A second analysis used a common 15 s window across all files. This sensitivity analysis checked whether the between-group differences depended on the duration of the analysed segment. In the 15 s analysis, the same duration was analysed for every participant. Because the length of the analysed time series may influence the estimation of nonlinear descriptors and complicate between-group comparisons, this sensitivity analysis was performed to determine whether the direction and magnitude of the between-group differences were maintained under equal-duration conditions (Mohammadzadeh Gonabadi & Burnfield, 2026).

The Python workflow was run twice, once with ANALYSIS_SECONDS = 30 and once with ANALYSIS_SECONDS = 15, and the results were exported to separate 30 s and 15 s folders.

The complete quality-control, processing and statistical comparison workflow is summarised in Figure 2.

2.7. Signal Preprocessing

For each triaxial sensor, the three axes were preprocessed separately. Each acceleration component was centred by subtracting its mean and then filtered using a fourth-order Butterworth low-pass filter with a 10 Hz cutoff frequency. The filter was applied forward and backward using filtfilt to achieve zero-phase filtering.

After centring and filtering, the three components were combined into a single triaxial acceleration magnitude according to Equation (1):

$$a_{dyn}(t) = \sqrt{x_f(t)^2 + y_f(t)^2 + z_f(t)^2} \quad (1)$$

where $x_f(t)$, $y_f(t)$, and $z_f(t)$ denote the corresponding centred and filtered acceleration components. In this study, $a_{dyn}(t)$ is operationally referred to as the dynamic acceleration magnitude.

All accelerometric descriptors included in the main analysis were derived from $a_{dyn}(t)$, rather than from the individual X, Y, and Z components.

2.8. Extracted Accelerometric Descriptors

For each participant, descriptors were calculated to characterise acceleration amplitude, rhythmicity, spectral content, and bilateral asymmetry. Time- and frequency-domain accelerometric features have previously been used to characterise gait and to distinguish between physiological and pathological walking patterns (Hsu et al., 2021; Sejdić et al., 2014). Global temporal organisation was assessed separately using DFA, as described in Section 2.10.

Acceleration amplitude was quantified using the root mean square (RMS) of each sensor's dynamic acceleration magnitude:

$$RMS = \sqrt{\frac{1}{N}\sum_{i=1}^{N} a_{dyn}(i)^2}. \quad (2)$$

The main rhythmic component of gait was estimated using the dominant frequency. Before spectral estimation, the dynamic acceleration magnitude was centred by subtracting its mean. Power spectral density was then estimated using Welch's method with a Hann window, 2048-sample segments, and 50% overlap between consecutive segments (Welch, 1967). For each signal, the dominant frequency was defined as the frequency bin corresponding to the maximum power spectral density within the predefined 0.4–3.0 Hz walking band.

To assess the relative contribution of higher-frequency components, a high-frequency ratio was calculated as the spectral power above 3 Hz and up to 10 Hz divided by the total spectral power within the 0.4–10 Hz interval:

$$R_{HF} = \frac{\int_{3}^{10} P(f)\,df}{\int_{0.4}^{10} P(f)\,df}, \quad (3)$$

where *P(f)* denotes the estimated power spectral density. Spectral power within both frequency intervals was calculated by trapezoidal numerical integration. The high-frequency ratio was treated as a study-specific spectral descriptor rather than as an established clinical index.

Left–right asymmetry was calculated between homologous sensor locations using their RMS values:

$$A_{RMS}(\%) = \frac{|RMS_L - RMS_R|}{(RMS_L + RMS_R)/2} \times 100. \quad (4)$$

A value of zero indicated identical RMS values on the two sides, whereas larger values indicated greater bilateral differences. Bilateral wearable-sensor measurements have previously been used to derive gait-asymmetry features (Anwary et al., 2018).

Separate sensor-level descriptors were calculated for the hip, knee, and ankle. Regional averaging and the calculation of combined knee–ankle descriptors are described in Section 2.11.

2.9. Estimation of Gait-Related Events and Accelerometric Cadence

Gait-related events were estimated separately from the dynamic acceleration magnitude signals recorded at the left and right ankles. Peak-based procedures have previously been used for gait-event and rhythm estimation from distal wearable sensors, although their implementation depends on sensor placement and signal characteristics (Anwary et al., 2018; Prasanth et al., 2021).

For each ankle, the signal was centred by subtracting its median. Peaks were detected using a minimum inter-peak distance of 0.30 s and a prominence threshold equal to 0.50 times the standard deviation of the corresponding signal.

The numbers of events detected at the left and right ankles were summed, and estimated cadence was calculated as

$$C_{est} = \frac{N_L + N_R}{T} \times 60, \quad (5)$$

where N_L and N_R denote the numbers of events detected at the left and right ankles, respectively, and T is the analysed duration in seconds. The resulting value was expressed in events per minute.

Because the detected peaks were not validated against an external gait-event reference, they were interpreted as estimated gait-related events rather than as confirmed heel strikes or toe-offs. Accordingly, the resulting cadence was treated as an accelerometric estimate of gait rhythm, not as a clinically validated gait-event detection or step-counting outcome.

2.10. Global DFA Analysis

Detrended Fluctuation Analysis (DFA) was applied to the dynamic acceleration magnitude of each sensor to estimate its global scaling behaviour (Peng et al., 1994). Because DFA estimates may be influenced by finite signal length, trends, and the selected range of scales, the same predefined scale interval was used for all participants and in both temporal analyses (Bashan et al., 2008; Bryce & Sprague, 2012).

Before analysis, non-finite values were removed, the signal was centred by subtracting its mean, and its cumulative profile was calculated. Twelve logarithmically spaced scales between 16 and 384 samples were used, corresponding to approximately 0.052–1.239 s at the effective system frame rate of approximately 310 frames/s.

At each scale, the cumulative profile was divided into non-overlapping segments. A first-order polynomial trend was fitted and removed within each segment, and the root mean square of the residuals was calculated. For each scale, the segment-level RMS residual fluctuations were combined using a root-mean-square calculation to obtain a single fluctuation value.

The global DFA exponent, denoted α_{DFA}, was obtained as the slope of the linear regression between the logarithm of the scales and the logarithm of the corresponding fluctuation values. The coefficient of determination, R^2, was also calculated for each sensor-level DFA fit.

In this study, α_{DFA} was interpreted as the scaling slope of the continuous dynamic acceleration magnitude over the predefined range of scales. It was not considered a diagnostic marker or a direct equivalent of the Hurst exponent derived from stride-interval time series.

2.11. Aggregation of Descriptors by Region

For each participant, sensor-level descriptors were initially calculated separately for the left and right sides. Bilateral regional values were subsequently obtained as the arithmetic mean of the corresponding measurements from homologous sensor locations. RMS values were aggregated at the hip, knee, and ankle levels, whereas dominant frequency, high-frequency ratio, and α_{DFA} were aggregated for the knee and ankle regions. Bilateral asymmetry remained a separate descriptor and was therefore not represented by these regional means.

For selected RMS, dominant frequency, and α_{DFA} outcomes, a combined knee–ankle value was calculated as the arithmetic mean of the corresponding regional knee and ankle values. This study-specific composite was used to summarise distal lower-limb accelerometric behaviour and was not considered an established clinical index.

The numerical variables included in the statistical analysis were age; total recording duration; analysed duration; RMS at the hip, knee, ankle, and combined knee–ankle levels; dominant frequency at the knee, ankle, and combined knee–ankle levels; high-frequency ratio at the knee and ankle levels; RMS asymmetry at the hip, knee, and ankle levels; estimated left, right, and total gait-related events; estimated cadence; and α_{DFA} at the knee, ankle, and combined knee–ankle levels.

Age, total duration, and analysed duration were treated as contextual variables or potential confounders, not as primary biomechanical descriptors.

2.12. Statistical Analysis

Statistical analyses were performed separately for the up-to-30-s and fixed 15-s datasets. Given the limited sample size and to avoid relying on assumptions of normality, continuous variables were summarised using the median and interquartile range (IQR).

Between-group comparisons were performed using the two-sided Mann–Whitney U test (Mann & Whitney, 1947). Effect size was quantified using Cliff's delta (Cliff, 1993), with the pathological group entered as the first group and the physiological group as the second. Positive Cliff's delta values therefore indicated higher values in the pathological group, whereas negative values indicated higher values in the physiological group.

Within each temporal analysis, the Benjamini–Hochberg false-discovery-rate procedure was applied jointly to the 22 numerical comparisons listed in Section 2.11 (Benjamini & Hochberg, 1995). The resulting FDR-adjusted p-values are reported as q-values, and $q < 0.05$ was considered statistically significant.

The absolute magnitude of Cliff's delta was classified as negligible ($|\delta| < 0.147$), small ($0.147 \leq |\delta| < 0.330$), medium ($0.330 \leq |\delta| < 0.474$), or large ($|\delta| \geq 0.474$). These values correspond closely to the rounded benchmarks of 0.15, 0.33, and 0.47 reported by Meissel and Yao (2024).

2.13. Temporal-Window Robustness Analysis

Results from the up-to-30-s and fixed 15-s analyses were subsequently merged by variable using a separate comparison script. The purpose of this analysis was to identify between-group contrasts that were robust across the two temporal configurations, rather than to demonstrate numerical stabilisation of individual descriptor values.

A between-group contrast was operationally classified as robust when all of the following conditions were met: $q < 0.05$ in the up-to-30-s analysis; $q < 0.05$ in the fixed 15-s analysis; the same sign of Cliff's delta in both analyses; and a large effect in both analyses, defined as $|\delta| \geq 0.474$. Contrasts that did not meet all four criteria were retained as secondary or exploratory findings.

The robustness criteria were evaluated for all numerical variables available in both temporal analyses. A predefined subset of ten accelerometric descriptors was retained for focused reporting: knee RMS, ankle RMS, combined knee–ankle RMS, ankle dominant frequency, combined knee–ankle dominant frequency, estimated cadence, knee asymmetry, ankle asymmetry, ankle α_{DFA}, and combined knee–ankle α_{DFA}. The focused subset was selected to represent the main descriptor categories while reducing redundancy between closely related regional measures. Distal measures were preferentially retained because acceleration recorded at the ankle reflects lower-limb advancement more directly and may better capture deviations in gait pattern. The subset was used only for focused reporting, while all numerical variables were included in the statistical and robustness analyses.

All preprocessing, descriptor extraction, quality-control procedures, statistical analyses, and figure generation were performed using custom Python scripts in Python 3.11.0rc2, with NumPy 2.4.6, pandas 3.0.3, SciPy 1.17.1, and Matplotlib 3.11.0.

3. Results

3.1. Participant and Recording Characteristics

The final analysis included 31 participants, of whom 15 belonged to the pathological gait group and 16 to the physiological gait group. The pathological group included 9 men and 6 women, whereas the physiological group included 8 men and 8 women. The pathological group had a higher median age than the physiological group, 59 [52–65] years compared with 48 [38.5–55.75] years. This age difference was considered a contextual factor and a potential confounder rather than a primary biomechanical finding.

Recordings obtained from the pathological group had a longer duration, with a median of 53.10 [41.12–58.98] s, compared with 28.49 [24.61–29.46] s in the physiological group. This difference reflected the longer time required by participants with pathological gait to complete the 30 m walking path.

Quality control did not lead to the exclusion of any recording. In the primary up-to-30-s analysis, 12 files from the pathological group were classified as GOOD and 3 as ACCEPTABLE. In the physiological group, 3 files were classified as GOOD and 13 as ACCEPTABLE. All 31 recordings were retained for the final analysis. Participant and recording characteristics are summarised in Table 1.

Table 1. Participant and recording characteristics

Characteristic	Pathological group	Physiological group
Participants (n)	15	16
Sex, M/F	9/6	8/8
Age, years	59 [52–65]	48 [38.5–55.75]
Total recording duration, s	53.10 [41.12–58.98]	28.49 [24.61–29.46]
QC: GOOD (n)	12	3
QC: ACCEPTABLE (n)	3	13
QC: REJECT (n)	0	0

Data are presented as median [IQR], unless otherwise indicated. M/F, male/female; QC, quality control.

3.2. Between-Group Differences in the Up-to-30-s Analysis

The primary analysis revealed clear between-group differences in acceleration amplitude, the dominant rhythmic component, estimated cadence, and bilateral asymmetry. The focused results from the up-to-30-s analysis are summarised in Table 2.

Table 2. Focused accelerometric descriptors and between-group comparisons in the up-to-30-s analysis.

Descriptor	Pathological group	Physiological group	q	Cliff's δ
Knee RMS, g	0.370 [0.307–0.551]	0.863 [0.737–0.952]	0.000307	−0.842
Ankle RMS, g	0.455 [0.358–0.506]	0.848 [0.804–0.902]	0.000223	−0.892
Knee–ankle RMS, g	0.425 [0.331–0.524]	0.846 [0.783–0.913]	0.000223	−0.883

Descriptor	Pathological group	Physiological group	q	Cliff's δ
Ankle dominant frequency, Hz	0.605 [0.530–0.757]	0.908 [0.908–0.908]	0.000223	−0.863
Knee–ankle dominant frequency, Hz	0.757 [0.568–0.757]	0.908 [0.908–0.908]	0.000458	−0.754
Estimated cadence, events/min	156.000 [129.000–173.000]	205.749 [196.363–221.674]	0.000363	−0.817
Knee RMS asymmetry, %	8.245 [3.187–24.436]	2.309 [0.803–3.965]	0.015121	0.550
Ankle RMS asymmetry, %	20.140 [8.692–25.271]	3.405 [1.321–4.072]	0.000458	0.792
Ankle αDFA	1.205 [1.198–1.207]	1.184 [1.163–1.205]	0.137136	0.333
Knee–ankle αDFA	1.170 [1.163–1.200]	1.162 [1.132–1.179]	0.067493	0.408

Data are presented as median [IQR]. Cliff's δ was calculated for the pathological-versus-physiological comparison; negative values indicate higher values in the physiological group, whereas positive values indicate higher values in the pathological group. DFA, Detrended Fluctuation Analysis; FDR, false discovery rate; IQR, interquartile range; RMS, root mean square.

In the up-to-30-s analysis, the physiological group had higher knee, ankle, and combined knee–ankle RMS values. Ankle and combined knee–ankle dominant frequencies and estimated accelerometric cadence were also higher in this group. In contrast, knee and ankle RMS asymmetry was greater in the pathological group. These differences remained significant after FDR correction and had large effect sizes (Table 2). No significant group differences remained after FDR correction for the high-frequency ratios or global DFA exponents.

3.3. Fixed 15-s Sensitivity Analysis

Repeating the analysis using the first 15 s of each recording preserved the main between-group differences. In this configuration, every participant contributed the same analysed signal duration, thereby removing the direct influence of unequal analysed segment lengths. The focused results from the fixed 15-s analysis, together with the robustness classification across temporal configurations, are summarised in Table 3.

Table 3. Focused accelerometric descriptors in the fixed 15-s analysis and robustness across temporal configurations.

Descriptor	Pathological group	Physiological group	q	Cliff's δ	Robust
Knee RMS, g	0.343 [0.276–0.524]	0.889 [0.742–1.009] g	0.000067	−0.900	Yes
Ankle RMS, g	0.407 [0.332–0.479]	0.873 [0.798–0.921] g	0.000048	−0.942	Yes
Knee–ankle RMS, g	0.397 [0.308–0.493]	0.866 [0.772–0.965] g	0.000056	−0.917	Yes
Ankle dominant frequency, Hz	0.605 [0.454–0.757]	0.908 [0.908–0.908]	0.000056	−0.858	Yes
Knee–ankle dominant frequency, Hz	0.719 [0.530–0.795]	0.908 [0.908–0.908]	0.000428	−0.733	Yes
Estimated cadence, events/min	128.000 [118.000–154.000]	226.000 [199.000–241.000]	0.000048	−0.942	Yes
Knee RMS asymmetry, %	9.858 [5.403–27.867]	1.575 [0.497–4.851]	0.007969	0.600	Yes
Ankle RMS asymmetry, %	19.859 [9.482–27.601]	3.254 [2.080–4.531]	0.000273	0.808	Yes
Ankle αDFA	1.197 [1.183–1.222]	1.165 [1.155–1.210]	0.113624	0.358	No

Descriptor	Pathological group	Physiological group	q	Cliff's δ	Robust
Knee–ankle αDFA	1.182 [1.156–1.201]	1.150 [1.120–1.177]	0.071463	0.408	No

Data are presented as median [IQR]. Cliff's δ was calculated for the pathological-versus-physiological comparison; negative values indicate higher values in the physiological group, whereas positive values indicate higher values in the pathological group. A contrast was classified as robust when $q < 0.05$ in both temporal analyses, the sign of Cliff's δ was the same, and $|\delta| \geq 0.474$ in both analyses. DFA, Detrended Fluctuation Analysis; FDR, false discovery rate; IQR, interquartile range; RMS, root mean square.

The fixed 15-s analysis showed the same general pattern as the up-to-30-s analysis. Knee, ankle, and combined knee–ankle RMS values were again higher in the physiological group. The same pattern was observed for ankle and combined knee–ankle dominant frequencies and estimated accelerometric cadence. In contrast, knee and ankle RMS asymmetry was higher in the pathological group (Table 3). No significant group differences were found for the high-frequency ratios or global DFA exponents after FDR correction.

3.4. Robust Between-Group Contrasts Across Temporal Configurations

Eight of the ten focused descriptors met all robustness criteria across both temporal windows: knee, ankle, and combined knee–ankle RMS; ankle and combined knee–ankle dominant frequency; estimated accelerometric cadence; and knee and ankle RMS asymmetry. Hip RMS and knee dominant frequency also showed robust contrasts outside the focused subset, whereas the two global DFA descriptors did not meet the robustness criteria.

Complete results for all numerical variables are provided in Table S1, with the corresponding machine-readable dataset available as Data S1.

4. Discussion

Acceleration amplitude, dominant rhythm, estimated cadence, and bilateral asymmetry showed the clearest group-level contrasts. However, these differences cannot be attributed exclusively to gait pathology. The groups were not age-matched, and walking speed was not measured independently. Still, the main contrasts retained the same direction and large effect sizes whether the analysis used an up-to-30-s window or a fixed 15-s window. Segment length alone, therefore, does not appear to explain the observed pattern.

The lower RMS values observed in the pathological group indicate a reduced amplitude of segmental acceleration during walking. These differences were present at the knee and ankle and were also preserved in the combined knee–ankle descriptor. Hip RMS, although not included in the focused set, also showed a robust between-group contrast. Hsu et al. (2021) similarly reported a significantly lower vertical trunk-acceleration RMS in participants after stroke than in healthy participants and showed that time-domain accelerometric features could contribute to gait-pattern differentiation. However, their study used a single inertial measurement unit (IMU) positioned at the lower back and analysed directional components, whereas the present study used the combined triaxial magnitude from sensors placed bilaterally at several lower-limb levels.

The lower RMS values should not be interpreted directly as reduced muscle force, mechanical power, or propulsion. None of these variables was measured in the present study. RMS describes the amplitude of the recorded acceleration magnitude and may be influenced by walking speed, movement range, sensor location, and the way in which motion is transmitted between body segments. These findings represent unadjusted group-level differences observed under self-selected walking conditions and do not isolate the influence of pathology from the potential effects of age or walking speed.

Dominant frequency and estimated cadence provided complementary information about gait rhythm. Both were lower in the pathological group, indicating a slower repetitive accelerometric pattern. This interpretation is also consistent with the longer time required by the pathological group to complete the 30 m walking path. Previous studies have shown that time- and frequency-domain

features derived from wearable sensors can distinguish physiological and pathological gait patterns (Hsu et al., 2021). Anwary et al. (2018) estimated cadence using distal sensors placed bilaterally. Without a conventional laboratory setup, they also extracted stride-related features and asymmetry data.

Nevertheless, the cadence reported here remains an accelerometric estimate. The detected peaks were not validated against force platforms, pressure insoles, or motion capture and were therefore not identified as confirmed heel strikes or toe-offs. The event counts and cadence should consequently be interpreted as descriptors of distal signal rhythm rather than as externally validated step-counting outcomes. The repeated dominant-frequency values observed in the physiological group also reflect, at least partly, the discrete frequency resolution of the Welch spectrum. Because dominant frequency was selected from predefined spectral bins, small differences in true gait rhythm may map to the same reported frequency value.

Bilateral asymmetry was greater in the pathological group, with the strongest difference observed at the ankle. This result suggests that pathological gait was characterised not only by lower acceleration amplitude and a slower rhythm but also by a less equal distribution of segmental acceleration between the two limbs. The bilateral sensor configuration was important in this respect because asymmetry cannot be described directly when the assessment is reduced to a single central signal. Anwary et al. (2018) demonstrated that synchronously recorded signals from both legs can be used to derive asymmetry and rhythm-related gait features. In clinical stroke rehabilitation, Felius et al. (2022) also found that many IMU-derived asymmetry features showed good-to-excellent test–retest reliability, supporting the potential clinical value of bilateral wearable measurements.

The more pronounced ankle asymmetry may reflect the distal expression of unequal limb advancement, foot control, or loading strategies. However, this interpretation remains indirect because joint angles, ground-reaction forces, plantar pressure, and muscle activity were not recorded. The present findings therefore support the ankle as an informative sensor location for detecting bilateral differences, but they do not establish which phase of gait or which biomechanical impairment generated those differences.

The use of six sensors also allowed the analysis to preserve regional information. A single trunk-mounted sensor can provide useful global measures and has practical advantages, but it cannot directly show whether a contrast is more evident proximally or distally. Wearable systems integrating IMUs with complementary sensing technologies can be evaluated against laboratory reference methods. Salis et al. (2023), for example, assessed a multi-sensor system combining IMUs, plantar-pressure insoles, and distance sensors against stereophotogrammetry. The present system was less complex than systems integrating inertial units, plantar-pressure insoles, and distance sensors, but it provided synchronous bilateral acceleration measurements at three lower-limb levels.

An important element of the study was the use of file-level quality control before descriptor extraction. No recording was excluded, but the distribution of GOOD and ACCEPTABLE files differed between groups. Most physiological recordings were classified as ACCEPTABLE because they were shorter than the nominal 30-s window, which resulted from participants completing the 30 m path more rapidly. This classification should not be interpreted as evidence of poorer signal quality in the physiological group. It reflects the operational QC definition, in which duration was considered together with structural and numerical integrity. The distinction illustrates why QC categories need to be interpreted in relation to the protocol rather than as general labels of measurement quality.

In contrast to RMS, dominant frequency, cadence, and asymmetry, the high-frequency ratio did not significantly differentiate the groups after FDR correction. This ratio was introduced as a study-specific descriptor to quantify the relative contribution of signal components above 3 Hz. Its lack of significance suggests that a consistent redistribution of spectral power toward higher frequencies was not a defining feature of the pathological group in this cohort. This may be related

to the heterogeneity of the pathological gait patterns, because different impairments may produce tremor-like components, impacts, compensatory movements, or smoother and slower motion in different proportions. It may also indicate that a single threshold at 3 Hz is too general to capture clinically relevant spectral differences across multiple sensor locations.

Global α_DFA did not significantly differentiate the two groups after FDR correction in either temporal analysis. This result should be considered in relation to both the signal analysed and the methodological properties of DFA. In the present study, DFA was applied to continuous segmental acceleration magnitude rather than to stride-interval series. The resulting exponent therefore does not represent the same physiological quantity as a conventional stride-interval DFA measure. Bashan et al. (2008) showed that the accuracy and uncertainty of the scaling exponent depend on signal length and the selected fitting range. They also demonstrated that trends and the detrending order can affect the observed scaling behaviour.

Data length is also relevant. Mohammadzadeh Gonabadi and Burnfield (2026) found that stabilisation requirements differed among nonlinear measures and reported no clear DFA stabilisation before the maximum available length of 3500 frames, corresponding to approximately 29.2 s. Their exploratory analysis was based on a single healthy participant during treadmill walking and motor-assisted elliptical exercise. The authors cautioned that the resulting stabilisation thresholds should not be generalised directly to pathological gait. Because the signal type, locomotor task, and study population also differ, their numerical findings cannot be transferred directly to the present overground, multi-segment accelerometry data.

For this reason, the fixed 15-s analysis in the present study was not intended to demonstrate numerical stabilisation of DFA or test-retest reliability. Its purpose was to determine whether the main between-group differences remained when the same signal duration was analysed for every participant. Eight of the ten focused descriptors met the predefined robustness criteria. In this cohort, RMS, dominant frequency, estimated accelerometric cadence, and bilateral asymmetry showed stronger and more readily interpretable group-level differences than global α_{DFA}.

5. Limitations

The study has several limitations. First, the sample was small, and the pathological group included participants with different neurological gait impairments. This clinical heterogeneity reflects rehabilitation practice but may have increased within-group variability and reduced the sensitivity of descriptors associated with specific diagnoses. In addition, no standardised measure of gait or functional impairment was administered. As a result, the severity of gait impairment could not be quantified or directly compared with the accelerometric descriptors.

Second, the pathological group was older than the physiological group. Age may influence walking speed, cadence, acceleration amplitude, and asymmetry, and the current study could not fully separate age-related effects from pathology-related effects. Anwary et al. (2018), for example, reported differences in walking duration and bilateral gait characteristics between younger and older groups, illustrating that age-related group differences may influence wearable-sensor outcomes.

Third, walking speed was self-selected and was not independently measured. Sekine et al. (2013) showed that trunk-acceleration RMS varied with preferred walking speed, while Hutin et al. (2012) demonstrated that changes in gait velocity affected cadence, spatiotemporal parameters, lower-limb kinematics, and intersegmental coordination in healthy and hemiparetic participants. Although these studies did not examine the exact multi-segment descriptors used here, they show that walking pace can influence both acceleration magnitude and gait organisation. Therefore, some of the observed differences may reflect both pathological gait characteristics and differences in self-selected pace. Because walking speed was not included as a covariate, and recording duration was not used as a substitute for a direct gait-speed measurement, the findings should be interpreted as unadjusted group differences observed under clinically realistic, self-selected walking conditions.

Fourth, the use of assistive devices may have contributed to the differences observed between the two groups. During the recorded trial, six of the 15 participants in the pathological

group used their usual walking aid. One used a cane and five used one forearm crutch each, all on the side opposite the affected limb. The remaining nine participants walked without an assistive device. This is relevant because walking aids may alter gait differently depending on the device and the population. Demir and Yildirim (2019) reported lower walking speed and cadence when adults with neuromuscular disease used a single-point cane, bilateral forearm crutches, or a walker than when they walked without an aid. Their protocol, however, included bilateral forearm crutches, whereas the participants in the present study used only one crutch. Härdi et al. (2014) found that canes, crutches, and walkers produced different changes in cadence, stride time and length, stride-length variability, double support, and gait speed among older habitual users. Jayakaran et al. (2014) also found that cane use for balance or partial weight support altered several temporal gait parameters in healthy adults. In the present study, assistive-device use was not standardised, and its effect was not examined separately. It is therefore not possible to determine how much of the observed differences were related to pathology, self-selected walking speed, or the walking aid itself.

Fifth, each participant contributed one walking recording, and no repeated-session reliability analysis was performed. Felius et al. (2022) showed that many IMU-derived gait features can be reliable in clinical stroke rehabilitation, but reliability is specific to the sensor configuration, protocol, feature definition, and population. The reliability of the descriptors generated by the GaitFlow Scanner therefore needs to be established directly in future studies.

Sixth, the system was not validated concurrently against an external biomechanical reference during the present protocol. The accelerometric results therefore cannot be treated as direct measurements of joint kinematics, gait phases, ground-reaction forces, or plantar loading. Carcreff et al. (2026) evaluated a multi-IMU system distributed across the pelvis and lower limbs against an optoelectronic motion-capture reference in participants with asymptomatic and heterogeneous pathological gait, illustrating the type of concurrent validation required before wearable-derived biomechanical outcomes can be interpreted at the individual level. The present study instead examined whether a comparatively simple six-sensor accelerometric configuration could generate consistent group-level contrasts using a common processing pipeline.

Future research should include larger and age-matched reference groups, as well as diagnosis-specific pathological cohorts. Recording walking speed and stratifying participants according to assistive-device use would help distinguish the influence of pathology from the influence of pace and external support. Repeated assessments are needed to determine test–retest reliability and minimal detectable change. Concurrent recording with motion capture, force platforms, or pressure insoles would also allow validation of the event-detection procedure and a more direct biomechanical interpretation of regional accelerometric differences.

Further methodological work could examine whether axis-specific signals, alternative spectral bands, or more localised and scale-resolved nonlinear measures provide information that is not captured by the global triaxial magnitude. The use of longer recordings may be particularly important for nonlinear analyses. Longitudinal studies could then determine whether the robust descriptors identified here are sensitive to changes during rehabilitation rather than only to differences between groups.

Taken together, the findings suggest that a quality-controlled, bilateral, multi-segment accelerometry pipeline can identify interpretable differences between physiological and pathological gait under a clinically feasible overground protocol. The strongest and most consistent information was provided by acceleration amplitude, rhythmicity, estimated cadence, and bilateral asymmetry. These descriptors should not yet be considered diagnostic biomarkers, but they provide a practical basis for further validation of wearable multi-segment gait assessment and for future monitoring of rehabilitation-related changes.

6. Conclusions

This study showed that a quality-controlled, bilateral, multi-segment accelerometry pipeline can identify interpretable differences between physiological and pathological gait during a clinically feasible overground walking protocol. The most consistent between-group contrasts were observed for acceleration amplitude, dominant frequency, estimated cadence, and bilateral RMS asymmetry. The physiological group showed higher RMS values, dominant frequencies, and estimated cadence, whereas the pathological group showed greater asymmetry at the knee and ankle. Because the groups were not age-matched, and walking speed was not independently measured, these contrasts cannot be attributed exclusively to gait pathology.

Eight of the ten descriptors selected for focused reporting remained significant after FDR correction, preserved the same direction of effect, and showed large effect sizes in both the up-to-30-s and fixed 15-s analyses. These findings indicate that the main group-level contrasts were not determined solely by unequal analysed signal durations. In contrast, the high-frequency ratio and global α_{DFA} did not provide significant group differentiation after FDR correction, suggesting that they were less consistent for group differentiation than the conventional amplitude, rhythm, and asymmetry measures in the present cohort and analytical configuration.

The results do not establish diagnostic biomarkers and should not be interpreted as direct measurements of gait biomechanics. However, they support the further development of multi-segment wearable accelerometry for clinical gait assessment. Larger, age-matched and diagnosis-specific cohorts, repeated measurements, and validation against external biomechanical references are required before the proposed descriptors can be used for individual clinical monitoring or rehabilitation outcome assessment.

7. Patents

The broader GaitFlow hardware–software platform associated with the system used in this study is the subject of Romanian patent application no. a 2025 00119, filed with the Romanian State Office for Inventions and Trademarks (OSIM) on 28 March 2025, under the title *"Portable Hardware Device with Dedicated Software for the Biomechanical Analysis of Gait, Running, or Sports-Related Physical Activities in Rehabilitation Medicine, Sports Medicine, and Medical Research."* At the time of manuscript preparation, the application was pending and scheduled for publication in the Official Industrial Property Bulletin, Inventions Section, No. 09/2026.

The GaitFlow figurative mark is registered with OSIM under trademark registration certificate no. 209282, with protection starting on 20 February 2025.

The associated software, officially registered as *"Gaitflow Analyzer,"* is recorded in the Romanian National Register of Works administered by the Romanian Copyright Office (ORDA) as a computer program under registration no. 870/04.03.2025.

Supplementary Materials: The following supporting information can be downloaded at the journal website: Table S1: Complete between-group comparisons for all numerical variables in the up-to-30-s and fixed 15-s analyses; Data S1: Machine-readable statistical comparison dataset for both temporal configurations.

Author Contributions: Conceptualisation, M.D.-A.; methodology, M.D.-A.; software, M.D.-A.; validation, M.D.-A.; formal analysis, M.D.-A.; investigation, M.D.-A.; resources, M.D.-A.; data curation, M.D.-A.; writing—original draft preparation, M.D.-A.; writing—review and editing, M.D.-A.; visualisation, M.D.-A.; project administration, M.D.-A. The author has read and agreed to the published version of the manuscript.

Funding: This research received no specific grant from any funding agency in the public, commercial, or not-for-profit sectors.

Institutional Review Board Statement: Ethical approval for the study was granted by the Ethics Committee of "Sf. Gheorghe" Rehabilitation Hospital, Botoșani, Romania, under approval no. 1 dated 14 February 2025. All study procedures were conducted in accordance with the principles of the Declaration of Helsinki.
Informed Consent Statement: Informed consent was obtained from all participants involved in the study.

Data Availability Statement: The aggregated data supporting the findings of this study are included in the article and its Supplementary Materials. Individual-level accelerometric recordings are not publicly available because of participant privacy and ethical considerations. De-identified participant-level data and the custom offline analysis scripts supporting the reported results may be made available by the corresponding author upon reasonable request, provided that the proposed use is compatible with the original ethical approval, participant consent, and applicable data-protection requirements. Firmware and proprietary software components associated with the GaitFlow platform are not included.

Acknowledgements: The author thanks the management and staff of "Sf. Gheorghe" Rehabilitation Hospital, Botoșani, Romania, for facilitating the clinical and organisational conditions required for data acquisition. The author also expresses his gratitude to Prof. Dorina-Emilia Creangă for the academic guidance provided within the doctoral research framework. During the preparation of this manuscript, the author used ChatGPT (OpenAI; accessed in 2026) for English translation and language editing, manuscript organisation and revision, and assistance with drafting and debugging portions of Python code. All AI-generated outputs were reviewed and edited by the author, who takes full responsibility for the content of the publication.

Conflicts of Interest: The author declares intellectual-property interests related to the GaitFlow platform, as described in Section 7. No other conflicts of interest are declared.

Abbreviations

The following abbreviations are used in this manuscript:

Abbreviation	Definition
DFA	Detrended Fluctuation Analysis
FDR	False Discovery Rate
IMU	Inertial Measurement Unit
IQR	Interquartile Range
QC	Quality Control
RMS	Root Mean Square

References

Anwary, A. R., Yu, H., & Vassallo, M. (2018). An automatic gait feature extraction method for identifying gait asymmetry using wearable sensors. *Sensors, 18*(2), Article 676. https://doi.org/10.3390/s18020676

Bashan, A., Bartsch, R., Kantelhardt, J. W., & Havlin, S. (2008). Comparison of detrending methods for fluctuation analysis. *Physica A: Statistical Mechanics and Its Applications, 387*(21), 5080–5090. https://doi.org/10.1016/j.physa.2008.04.023

Benjamini, Y., & Hochberg, Y. (1995). Controlling the false discovery rate: A practical and powerful approach to multiple testing. *Journal of the Royal Statistical Society: Series B (Methodological), 57*(1), 289–300. https://doi.org/10.1111/j.2517-6161.1995.tb02031.x

Bryce, R. M., & Sprague, K. B. (2012). Revisiting detrended fluctuation analysis. *Scientific Reports, 2*, Article 315. https://doi.org/10.1038/srep00315

Carcreff, L., Payen, G., Grouvel, G., Cardoso-Fonseca, M., Massé, F., & Armand, S. (2026). Validity, reliability and interpretability of an IMU-based system to measure 3D lower limb kinematics of patients with heterogeneous gait disorders. *Sensors, 26*(6), Article 1746. https://doi.org/10.3390/s26061746

Chen, S., Lach, J., Lo, B., & Yang, G.-Z. (2016). Toward pervasive gait analysis with wearable sensors: A systematic review. *IEEE Journal of Biomedical and Health Informatics, 20*(6), 1521–1537. https://doi.org/10.1109/JBHI.2016.2608720

Cliff, N. (1993). Dominance statistics: Ordinal analyses to answer ordinal questions. *Psychological Bulletin, 114*(3), 494–509. https://doi.org/10.1037/0033-2909.114.3.494

Demir, Y. P., & Yildirim, S. A. (2019). Different walk aids on gait parameters and kinematic analysis of the pelvis in patients with adult neuromuscular disease. *Neurosciences, 24*(1), 36–44. https://doi.org/10.17712/nsj.2019.1.20180316

Díaz, S., Stephenson, J. B., & Labrador, M. A. (2020). Use of wearable sensor technology in gait, balance, and range of motion analysis. *Applied Sciences, 10*(1), Article 234. https://doi.org/10.3390/app10010234

Dobîndă-Albu, M. (2026). AI-enhanced gait re-education: Overcoming linguistic and cultural barriers in rehabilitation. *BRAIN. Broad Research in Artificial Intelligence and Neuroscience, 17*(2), 282–300. https://doi.org/10.70594/brain/17.2/17

Felius, R. A. W., Geerars, M., Bruijn, S. M., van Dieën, J. H., Wouda, N. C., & Punt, M. (2022). Reliability of IMU-based gait assessment in clinical stroke rehabilitation. *Sensors, 22*(3), Article 908. https://doi.org/10.3390/s22030908

Goldberger, A. L., Amaral, L. A. N., Hausdorff, J. M., Ivanov, P. C., Peng, C.-K., & Stanley, H. E. (2002). Fractal dynamics in physiology: Alterations with disease and aging. *Proceedings of the National Academy of Sciences of the United States of America, 99*(Suppl. 1), 2466–2472. https://doi.org/10.1073/pnas.012579499

Härdi, I., Bridenbaugh, S. A., Gschwind, Y. J., & Kressig, R. W. (2014). The effect of three different types of walking aids on spatio-temporal gait parameters in community-dwelling older adults. *Aging Clinical and Experimental Research*, *26*, 221–228. https://doi.org/10.1007/s40520-014-0204-4

Hausdorff, J. M. (2007). Gait dynamics, fractals and falls: Finding meaning in the stride-to-stride fluctuations of human walking. *Human Movement Science, 26*(4), 555–589. https://doi.org/10.1016/j.humov.2007.05.003

Hausdorff, J. M., Peng, C.-K., Ladin, Z., Wei, J. Y., & Goldberger, A. L. (1995). Is walking a random walk? Evidence for long-range correlations in stride interval of human gait. *Journal of Applied Physiology, 78*(1), 349–358. https://doi.org/10.1152/jappl.1995.78.1.349

Hsu, W.-C., Sugiarto, T., Liao, Y.-Y., Lin, Y.-J., Yang, F.-C., Hueng, D.-Y., Sun, C.-T., & Chou, K.-N. (2021). Can trunk acceleration differentiate stroke patient gait patterns using time- and frequency-domain features? *Applied Sciences, 11*(4), Article 1541. https://doi.org/10.3390/app11041541

Hutin, E., Pradon, D., Barbier, F., Bussel, B., Gracies, J.-M., & Roche, N. (2012). Walking velocity and lower limb coordination in hemiparesis. *Gait & Posture, 36*(2), 205–211. https://doi.org/10.1016/j.gaitpost.2012.02.016

Jayakaran, P., DeSouza, L., Cossar, J., & Gilhooly, K. (2014). Influence of a walking aid on temporal and spatial parameters of gait in healthy adults. *PM&R, 6*(9), 796–801. https://doi.org/10.1016/j.pmrj.2014.02.005

Mann, H. B., & Whitney, D. R. (1947). On a test of whether one of two random variables is stochastically larger than the other. *The Annals of Mathematical Statistics, 18*(1), 50–60. https://doi.org/10.1214/aoms/1177730491

Meissel, K., & Yao, E. S. (2024). Using Cliff's delta as a non-parametric effect size measure: An accessible web app and R tutorial. *Practical Assessment, Research, and Evaluation, 29*, Article 2. https://doi.org/10.7275/pare.1977

Mohammadzadeh Gonabadi, A., & Burnfield, J. M. (2026). Effect of data length on nonlinear analysis of human motion during locomotor activities. *Applied Sciences, 16*(8), Article 3939. https://doi.org/10.3390/app16083939

Peng, C.-K., Buldyrev, S. V., Havlin, S., Simons, M., Stanley, H. E., & Goldberger, A. L. (1994). Mosaic organization of DNA nucleotides. *Physical Review E, 49*(2), 1685–1689. https://doi.org/10.1103/PhysRevE.49.1685

Phinyomark, A., Larracy, R., & Scheme, E. (2020). Fractal analysis of human gait variability via stride interval time series. *Frontiers in Physiology, 11*, Article 333. https://doi.org/10.3389/fphys.2020.00333

Prasanth, H., Caban, M., Keller, U., Courtine, G., Ijspeert, A., Vallery, H., & von Zitzewitz, J. (2021). Wearable sensor-based real-time gait detection: A systematic review. *Sensors, 21*(8), Article 2727. https://doi.org/10.3390/s21082727

Salis, F., Bertuletti, S., Bonci, T., Caruso, M., Scott, K., Alcock, L., Buckley, E., Gazit, E., Hansen, C., Schwickert, L., Aminian, K., Becker, C., Brown, P., Carsin, A.-E., Caulfield, B., Chiari, L., D'Ascanio, I., Del Din, S., … Mobilise-D Consortium. (2023). A multi-sensor wearable system for the assessment of diseased gait in real-world conditions. *Frontiers in Bioengineering and Biotechnology, 11*, Article 1143248. https://doi.org/10.3389/fbioe.2023.1143248

Sejdić, E., Lowry, K. A., Bellanca, J., Redfern, M. S., & Brach, J. S. (2014). A comprehensive assessment of gait accelerometry signals in time, frequency and time-frequency domains. *IEEE Transactions on Neural Systems and Rehabilitation Engineering, 22*(3), 603–612. https://doi.org/10.1109/TNSRE.2013.2265887

Sekine, M., Tamura, T., Yoshida, M., Suda, Y., Kimura, Y., Miyoshi, H., Kijima, Y., Higashi, Y., & Fujimoto, T. (2013). A gait abnormality measure based on root mean square of trunk acceleration. *Journal of NeuroEngineering and Rehabilitation, 10*, Article 118. https://doi.org/10.1186/1743-0003-10-118

Welch, P. D. (1967). The use of fast Fourier transform for the estimation of power spectra: A method based on time averaging over short, modified periodograms. *IEEE Transactions on Audio and Electroacoustics, 15*(2), 70–73. https://doi.org/10.1109/TAU.1967.1161901